ARTICLES

Detailed Mechanism for Trans−Cis Photoisomerization of Butadiene Following a Femtosecond-Scale Laser Pulse

Yusheng Dou,[†] Ben R. Torralva,[‡] and Roland E. Allen*[,†]

Physics Department, Texas A&M University, College Station, Texas 77843, and Chemistry and Materials Science, Lawrence Livermore National Laboratory, California 94550

Received: March 26, 2003; In Final Form: August 7, 2003

The detailed dynamical processes involved in trans → cis photoisomerization of butadiene have been studied in realistic simulations, employing a technique that is described in the text. Many interesting features are observed, including the following sequence of events: (i) The initial electronic excitation converts the central single bond to a double bond and the terminal double bonds to single bonds, so the molecule at first rotates about only these end bonds. (ii) There is then a series of rapid nonadiabatic transfers of population among electronic states near the HOMO−LUMO gap, which ultimately result in depopulation of the excited states. (iii) The bonds consequently revert to their original ground-state character, permitting a continuous rotation about the central single bond. At the end, the molecule is essentially in the ground electronic state for the new conformation. The simulation results clearly demonstrate the couplings of C−C−C bending vibrations to nonadiabatic electronic transitions and involvement of hydrogen migration in the molecular orbital intersections.

I. Introduction

The photoisomerization of linear polyenes has an important place among chemical and biological reactions.[1−4] Examples are the primary vision event in retinal, the chromophore of rhodopsin,[5−7] and similar events in vitamin D compounds.[8] There have been many experimental and theoretical investigations of this general topic.

Three electronic states are involved in the photoisomerization of polyenes: the ground state 1^1A_g; the ionic state 1^1B_u, corresponding to the dipole-allowed HOMO → LUMO one-electron excitation; the covalent excited state 2^1A_g, corresponding to dipole-forbidden excitations in the usual one-photon sense, including HOMO − 1 → LUMO, HOMO → LUMO + 1, and $HOMO^2 \rightarrow LUMO^2$. One of the proposed mechanisms for very short polyenes, including 1,3-butadiene (hereafter called butadiene), is that isomerization starts from the 1^1B_u state, then switches to the 2^1A_g state via an internal conversion process, and finally goes to the ground state 1^1A_g through a conical intersection. The reaction ends with either the product or reactant in the ground state.

Experimental investigations aim at probing the locations and ordering of electronically excited states, and the vibrational couplings among the relevant electronic states, using a variety of spectroscopic techniques, including absorption,[9,10] fluorescence,[11−13] electron energy loss,[14] and resonance Raman[15,16] spectroscopies. The development of ultrashort laser pulses has stimulated numerous experimental investigations of the photoisomerization dynamics of polyenes.[17−21] A significant achievement in this area is the discovery, using differential absorption spectra,[17] that the 11-cis to all-trans torsional isomerization of retinal in rhodopsin is essentially completed in only 200 fs. Recently, a nonresonant multphoton ionization experiment has demonstrated that trans → cis isomerization of butadiene proceeds within about 420 fs.[20] Theoretical approaches attempt to provide a detailed knowledge of the potential energy surfaces of the ground and electronically excited states as a tool for understanding the isomerization reaction paths.[22−30] Semiclassical molecular dynamics calculations have been frequently used to study the photoisomerization dynamics of polyenes.[31−43] Some early calculations were based on a one-dimensional approximation (torsion mode only).[22,23] These calculations provide a fairly comprehensive picture of the role of the C−C single bond but are unable to fully reveal the detailed mechanisms and irreversible nature of the reaction.

Recently, efforts have been made to simulate the events over a larger conformational space of internal coordinates: Using a vibronic-coupling model, Krawczyk et al. examined the nonadiabatic coupling between the two low-lying electronically excited states, 1^1B_u and 2^1A_g, in the vicinity of the equilibrium geometry of the electronic ground state,[37] and their study includes the most relevant active vibrational modes. Ito and Ohmine employed a parametrized model Hamiltonian and surface-hopping scheme to study the *trans*-butadiene photoisomerization process with a partial set of atomic degrees of freedom, including C−C bond stretching, bond bending, and torsions.[38] Utilizing a molecular mechanics force field and valence bond theory, Robb and co-workers investigated the electronic excited-state dynamics of *trans*-butadiene[39] and other polyenes with longer chains.[40]

[†] Texas A&M University.
[‡] Lawrence Livermore National Laboratory.

10.1021/jp034771b CCC: $25.00
Published on Web 09/25/2003

These studies reveal the complexity of the process. For detailed understanding of the photoisomerization dynamics of polyenes, it is necessary to include all atomic degrees of freedom and compute atomic forces "on the fly" as the system propagates along its trajectory. It appears that this kind of calculation has only been employed in a study of the cis → trans photoisomerization of ethylene (the basic polyene unit) by the group of Martínez.[41]

In the past, semiclassical simulations have been taken to start from a configuration in which a single electron is vertically promoted to a single excited state. However, in a real laser pulse experiment,[44] the electronic configuration is one in which various excited states are occupied with various amplitudes. These amplitudes depend not only on the electronic structure of the target molecule but also on the properties of the laser pulse, including the wavelength, fluence, and duration. Furthermore, as will be seen below, an ultraintense laser pulse may produce transitions from one excited state to another. The electronic configuration of a molecule under laser irradiation may therefore be significantly different from one based on simplistic energy surfaces. The same is true of the nuclear motion, because the electronic state determines the forces on the nuclei.

With the above motivation, we have developed a method for simulating the response of molecules to laser pulses[45−48] that is realistic in the present context and that can be extended to other types of reactions.[46] This method is described in the next section. The results for *trans*-butadiene → *cis*-butadiene are presented in section 3, and a summary is given in section 4.

II. Methodology

The general method used here is called semiclassical electron−radiation−ion dynamics (SERID) to emphasize both its strengths and its limitations. The valence electrons are treated quantum-mechanically, but both the radiation field and the motion of the ion cores are treated classically (this is not as severe a limitation as it may first appear to be, because a semiclassical treatment in time-dependent perturbation theory still gives effective *n*-photon and *n*-phonon processes in absorption and stimulated emission). In the version of the method used here, the one-electron Hamiltonian **H** has a semiempirical form, but the values of the parameters determining both **H** and the ion−ion repulsion were determined in the density-functional calculations of Frauenheim and co-workers.[49] These parameters were found to give a remarkably good description of C_{60} responding to laser pulses of various intensities, ranging from low to very high.[47] The description of the C−H bond is also quite accurate, so it is clear that this model is quite suitable for butadiene, the subject of the present paper.

The most severe limitation of the present method is that it is based on a mean-field picture, which inherently neglects many-body effects. The electronically excited states are thus not treated accurately, and this is particularly true of the 2^1A_g state. However, the present method provides a detailed dynamical picture that is complementary to the simpler pictures used in more accurate quantum calculations.

Our method is designed to treat the forces on the atomic nuclei (or ion cores) when there are multiple electronic excitations with the wave functions updated at every time step via solution of the time-dependent Schrödinger equation

$$i\hbar \frac{\partial \mathbf{\Psi}_j}{\partial t} = \mathbf{S}^{-1}\cdot\mathbf{H}\cdot\mathbf{\Psi}_j \qquad (1)$$

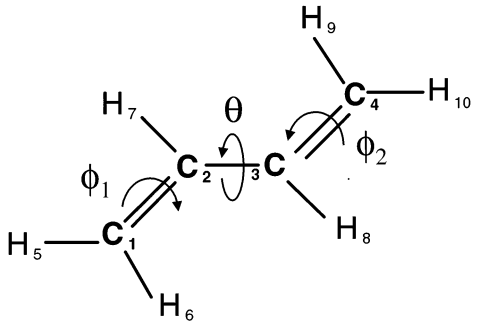

Figure 1. Definitions of internal coordinates for *trans*-butadiene.

where **S** is the overlap matrix for the atomic orbitals. The time-dependent vector potential for the radiation field is coupled to the electronic Hamiltonian via the Peierls substitution

$$H_{ab}(\mathbf{X}-\mathbf{X}') = H^0_{ab}(\mathbf{X}-\mathbf{X}')\exp\left(\frac{iq}{\hbar c}\mathbf{A}(t)\cdot(\mathbf{X}-\mathbf{X}')\right) \qquad (2)$$

where **X** and **X′** are nuclear coordinates, *a* and *b* label atomic orbitals, **A**(*t*) is the vector potential for the radiation field, and $q = -e$ is the charge of the electron. Equation 2 respects gauge invariance, requires no new parameters, and is applicable to strong time-dependent electromagnetic fields. The basic idea was introduced by Peierls in 1933[50] for static fields, was later generalized to time-dependent fields by Graf and Vogl,[51] and was subsequently discussed by Boykin et al.[52] In the present context, the Peierls substitution provides a proper treatment of the laser excitation process with the laser pulse having its specific properties, including wavelength, fluence, and duration. With a classical treatment of the radiation field, spontaneous emission is omitted. However, spontaneous emission, like other vacuum effects, is relatively weak and does not significantly affect the short-time-scale dynamics of butadiene emphasized in the present study.

The motion of the nuclei (or ion cores) is determined by Ehrenfest's theorem

$$M_l\frac{d^2X_{l\alpha}}{dt^2} = -\frac{1}{2}\sum_j \mathbf{\Psi}_j^\dagger\cdot\left(\frac{\partial \mathbf{H}}{\partial X_{l\alpha}} - i\hbar\frac{\partial \mathbf{S}}{\partial X_{l\alpha}}\frac{\partial}{\partial t}\right)\cdot\mathbf{\Psi}_j + \text{h.c.} - \frac{\partial U_{rep}}{\partial X_{l\alpha}} \qquad (3)$$

which can also be interpreted as a generalized Hellmann−Feynman theorem. Equation 3 is numerically solved with the velocity Verlet algorithm (which preserves phase space), and eq 1 is solved with an improved Cayley algorithm developed by Graves and Torralva[45] (which conserves probability and ensures that the Pauli principle always holds). A time step of 50 as was used because it was found to give converged results in test runs.

Before the laser field is applied, the *trans*-butadiene molecule is given 1000 fs to relax to its ground-state geometry, which is found to be in agreement with experiment.[53] The internal coordinates are defined in Figure 1. The three torsional angles, θ, ϕ_1, and ϕ_2, defined by $C_1-C_2-C_3-C_4$, $H_6-C_1-C_2-C_3$, and $C_2-C_3-C_4-H_{10}$, respectively, are 180°, 0°, and −180° in the equilibrium geometry for the electronic ground state. The laser pulse was taken to have a full width at half-maximum (fwhm) duration of 75 fs (with a Gaussian profile), a wavelength corresponding to 4.18 eV, and a fluence of 0.90 kJ/m^2. This wavelength matches the energy gap between the HOMO and LUMO orbitals of *trans*-butadiene calculated with the density functional approach. The fluence was chosen such that the forces

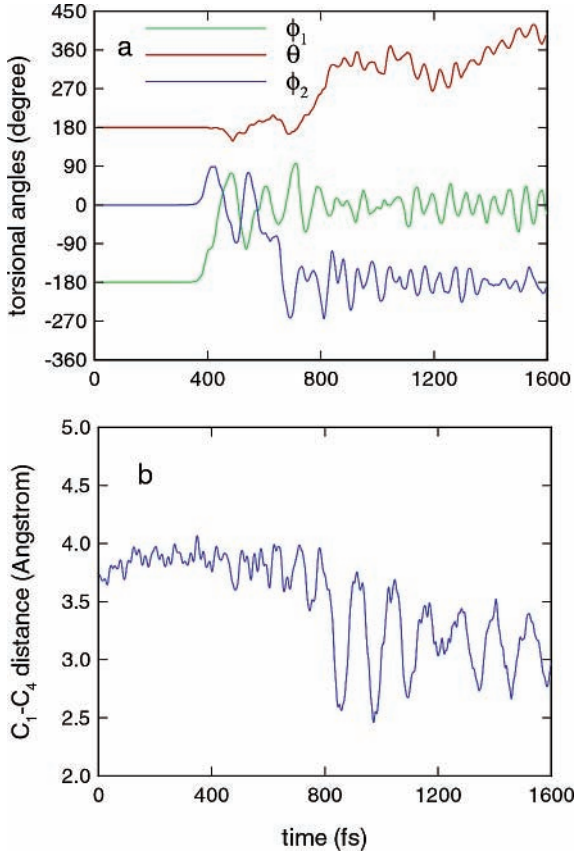

Figure 2. Variations with time of (a) the torsional angles θ, ϕ_1, and ϕ_2 defined in Figure 1 and (b) C_1-C_4 intramolecular distance in butadiene.

on the nuclei are large enough to produce a change of geometry but not a dissociative reaction. A similar laser pulse was used in the experiments of Fuss and co-workers.[20]

III. Results and Discussion

In this section, we first present results for the trans → cis photoisomerization of butadiene and then use these results to understand the detailed photoisomerization mechanism. The variations with time of the torsional angles θ, ϕ_1, and ϕ_2 are presented in Figure 2a. Figure 2b shows the separation of the two carbon atoms at the ends of the molecule, again as a function of time.

First consider the torsional angle variations in Figure 2a, in which one can observe that the butadiene twists actively about the two terminal C−C bonds after 380 fs but exhibits a large rotation about the central bond only after about 700 fs. Starting from 180°, θ increases to approximately 360° by 900 fs and then fluctuates about this angle. On the other hand, ϕ_1 starts from −180°, reaches 0° at around 450 fs, and then maintains this geometry; ϕ_2, initially at 0°, reaches −180° at about 700 fs and then stays near this angle until the end of the simulation. These results indicate that the cis conformation is achieved about 900 fs after the laser pulse is applied.

Another direct indication of the formation of the cis structure is provided by the distance between the two terminal carbon atoms, C_1 and C_4, which evolves from about 3.8 Å (in the initial trans form) to about 3.0 Å (in the final cis form) over a period of about 900 fs, as can be seen in Figure 2b.

The changes in the energies of the HOMO, LUMO, and LUMO + 1 and the time-dependent populations of the LUMO and LUMO + 1 are presented in Figure 3, panels a and b,

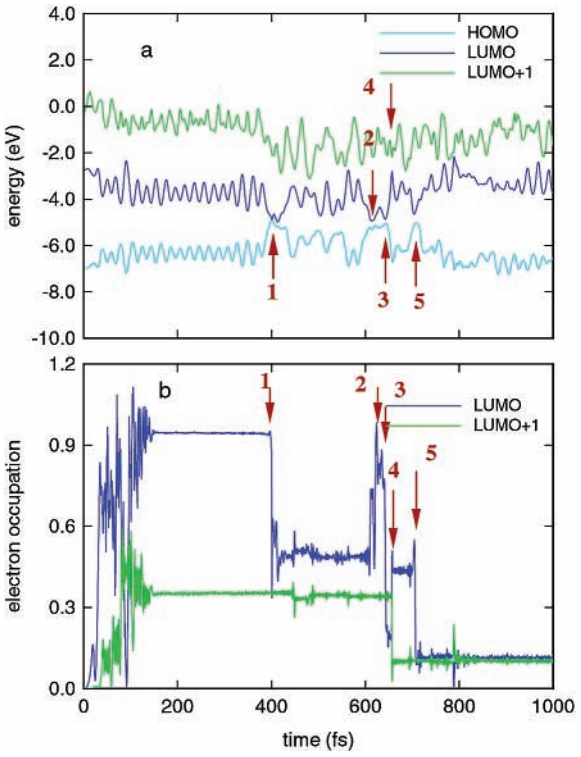

Figure 3. Variations with time (a) of HOMO, LUMO, and LUMO + 1 orbital energies. Note the five near-crossings indicated by red arrows. Panel b shows the electron occupancy of LUMO and LUMO + 1 orbitals. Note the five nonadiabatic transitions, which result from the five near-crossings and which are also marked by red arrows.

respectively. Expanded versions of the Figure 3 scales, from 0 to 150 fs (a period corresponding to the laser excitation process), are shown in Figure 4. At the end of the laser pulse, approximately 0.95 electrons have been excited to the LUMO (from the HOMO) and 0.35 electrons to the LUMO + 1. Less than 0.05 electrons reach the molecular orbitals above the LUMO + 1, and these electrons will therefore not be discussed any further. The excitation to the LUMO + 1 is mainly out of the LUMO at around 85 fs, when the energy gap between the two orbitals matches the wavelength of the radiation, as can be seen in Figure 4.

With the further progression of time, several strong couplings develop between the three relevant molecular orbitals, as can be observed in Figure 3a. From about 400 to 710 fs, there are five such couplings, labeled 1, 2, ..., 5. These are found to produce rapid nonadiabatic electronic transitions, leading to dramatic changes in the occupation numbers of the LUMO and LUMO + 1 orbitals, which are also labeled 1, 2, ..., 5, in Figure 3b. The energy gaps of the five nonadiabatic couplings are 0.01 eV for 1, 0.29 eV for 2, 0.17 eV for 3, 0.65 eV for 4, and 0.45 eV for 5.

It can be seen in Figure 3 that the nonadiabatic couplings 1, 3, and 5, occurring at 402, 643, and 705 fs, respectively, induce electronic transitions from LUMO to HOMO. Also, the level interaction 4 at 656 fs induces a transition from LUMO + 1 to LUMO. On the other hand, level interaction 2 at 618 fs leads to an upward transition from HOMO to LUMO. After 705 fs, the energy gap between HOMO and LUMO increases to about 4.0 eV (the value at around 800 fs) and then remains at this value until the end of the simulation.

It has been demonstrated[24,28] that a low-energy electronic excited state and the ground state become degenerate at a conformation where three C−C bonds are partially twisted. A general nuclear trajectory will, of course, not pass through

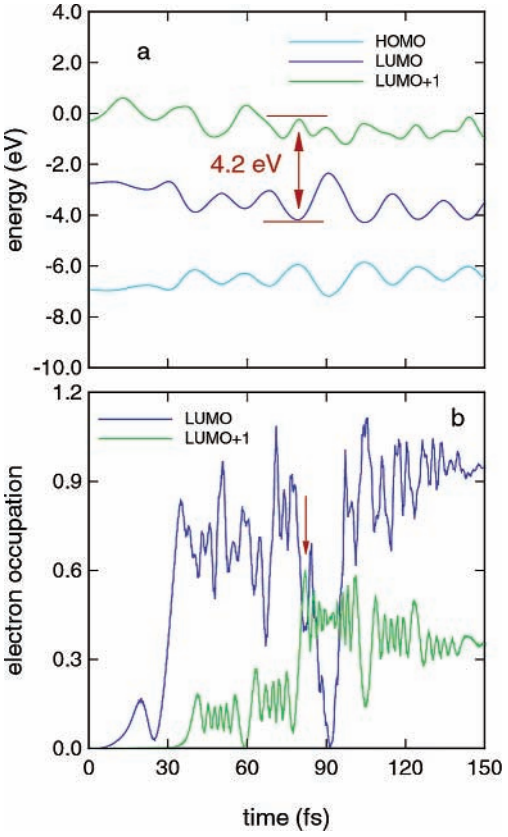

Figure 4. Expanded scale for (a) Figure 3a and (b) Figure 3b from 0 to 150 fs, the full duration of the applied laser pulse.

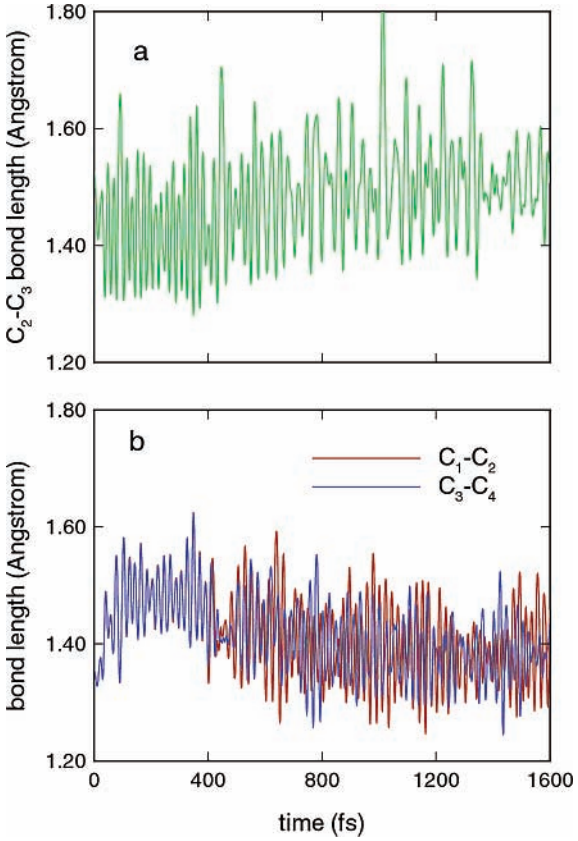

Figure 5. Variation with time in (a) C_2-C_3 bond length and (b) C_1-C_2 and C_3-C_4 bond lengths.

the exact point of this degeneracy, or conical intersection, but may pass nearby and induce a near-degeneracy, or avoided crossing.

Figure 3 demonstrates that all nonadiabatic transitions occur at such avoided crossings. We observe that (i) nonadiabatic couplings occur over a wide range of C−C torsional angles and (ii) quite efficient transitions from LUMO to HOMO, or from LUMO + 1 to LUMO, occur with an energy gap as large as 0.65 eV. These results indicate that isomerization does not require the system to follow an energy minimum. This conclusion was also reached in a molecular dynamics study of the photoisomerization of *cis*-stilbene by Berweger et al.[43] They observed that relaxation of excited *cis*-stilbene does not take place at the primary gauche minimum in energy.

Our observation that the molecule starts to twist about its two terminal C−C bonds after application of the laser pulse and before the first nonadiabatic electronic transition indicates that this initial torsional motion is caused by redistribution of energy from other vibrational modes that are activated when electrons are promoted to excited states. The later torsional motion of the central C−C bond, on the other hand, is clearly activated by energy released in the nonadiabatic transition at 405 fs.

Simulations starting from the same initial molecular geometry but with a slightly different fluence or wavelength for the laser pulse reveal slight variations in both the precise times of the avoided crosses and the values of the associated energy gaps. As a result, the transition rates for the electrons at these avoided crosses are also found to vary. These differences are interpreted as arising from differences in the occupation of the molecular orbitals, which in turn result from differences in the laser pulse parameters and which lead to differences in the forces responsible for nuclear motion. However, in all cases, there were gaps characteristic of avoided crossings, and we did not observe a tendency toward energy degeneracy of the HOMO and LUMO. In addition, no noticeable change was observed in the molecular twisting pattern around the three C−C bonds from that presented here. When the fluence or wavelength of the laser pulse was further increased, some simulations led to a dissociation reaction involving C−C bonds and some to a substantially prolonged lifetime for the excited *cis*-butadiene.

The variations with time of the central and two terminal C−C bond lengths are shown in Figure 5. Upon excitation of electrons to the LUMO level and further excitation to the LUMO + 1, an effective inversion of the characters of the C−C double and single bonds is observed: As can be seen in Figure 5, the central C−C bond length decreases from 1.5 Å to an average of 1.4 Å, whereas the two terminal C−C bond lengths increase from 1.35 Å to an average of 1.48 Å. This effect is due to electron redistribution resulting from excitation. We also find that the frequency of the C−C stretching motion increases for the central bond and decreases for the two terminal bonds. This change in vibrational frequencies is, of course, consistent with the changes in bond lengths. Finally, the amplitudes of the stretching motions for both central and terminal C−C bonds are found to be larger in the electronically excited state because the abrupt change in force constants indirectly leads to vibrational excitation of these modes.

After the nonadiabatic decays at 405, 643, 656, and 705 fs, all three C−C bonds revert to their normal ground-state lengths and vibrational frequencies but retain large vibrational amplitudes, as is evident in Figure 5. The further enhancement in vibrational amplitude of the two terminal C−C bonds after about 600 fs indicates the strong coupling of the symmetric stretching motion of these bonds to the nonadiabatic transition, as has also been suggested by studies using ab initio approaches.[23,30]

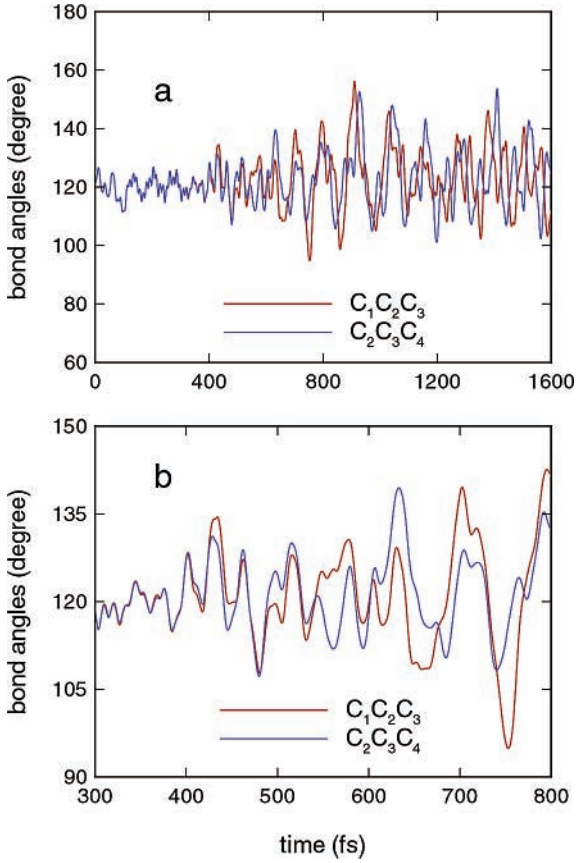

Figure 6. $C_1-C_2-C_3$ and $C_2-C_3-C_4$ bond-bending angles (a) as functions of time and (b) expanded scale for panel a.

Variations with time of two C−C−C bond-bending angles are shown in Figure 6a, and an expanded view from 300 to 800 fs is given in Figure 6b. One can immediately see, in Figure 6a, that these C−C−C bending modes exhibit similar features: Both are significantly activated after 400 fs and further intensified after 700 fs. However, more detailed examination reveals (in Figure 6b) that there is a subtle distinction during the period from 600 to 800 fs: At about 400 fs, both bending vibrations promote nonadiabatic coupling. Both also accept the energy that is consequently released, as evidenced by the enhancement in their vibrational amplitudes at this point. Later, at about 640 fs, the $C_2-C_3-C_4$ bending vibration stimulates a nonadiabatic transition from HOMO to LUMO but without an increase in its vibrational amplitude. On the other hand, the $C_1-C_2-C_3$ bending vibration does accept kinetic energy after it couples to a nonadiabatic transition, from LUMO to HOMO, at 700 fs. The importance of C−C−C in-plane bending vibrations as a source of nonadiabatic coupling has also been discussed in refs 23 and 30.

Let us now consider the effects of hydrogen migration on nonadiabatic couplings. In Figure 7, we show the behavior of the $C_1-C_2-H_7$ and $C_4-C_3-H_8$ bending angles and the C_2-H_7 and C_3-H_8 bond lengths, during the photoisomerization process. In Figure 8, the $C_4-C_3-H_8$ bending angle and C_3-H_8 bond length are shown from 580 to 760 fs on an expanded scale.

It can be seen in Figure 7 that these C−C−H bending modes and central C−H stretching modes are excited by laser irradiation. The further enhancement of $C_1-C_2-H_7$ bending vibrations immediately after 700 fs (in Figure 7a) is a consequence of the nonadiabatic electronic transition at 705 fs. It can be seen in Figure 7b that there are several distinct processes that cause energy to flow in to and out of the stretching modes for the two central C−H bonds.

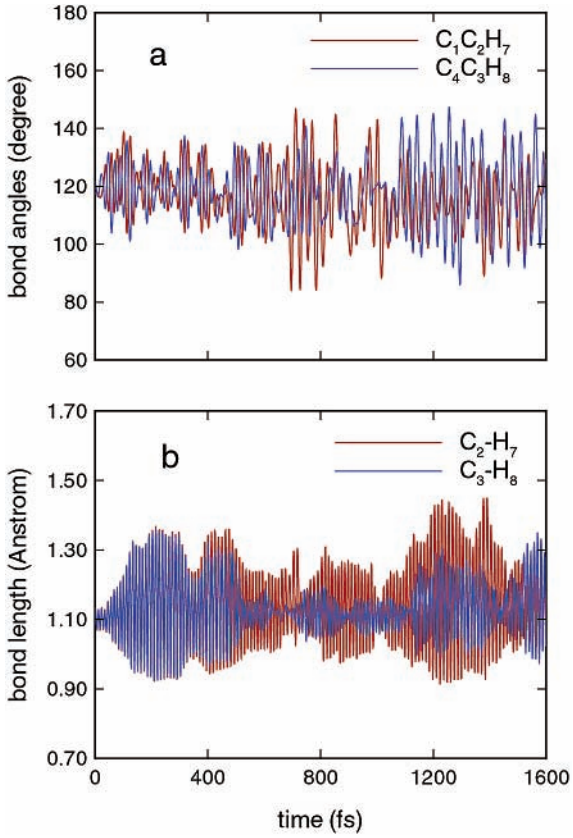

Figure 7. Variations of (a) $C_1-C_2-H_7$ and $C_4-C_3-H_8$ bond-bending angles and (b) C_2-H_7 and C_3-H_8 bond length as functions of time.

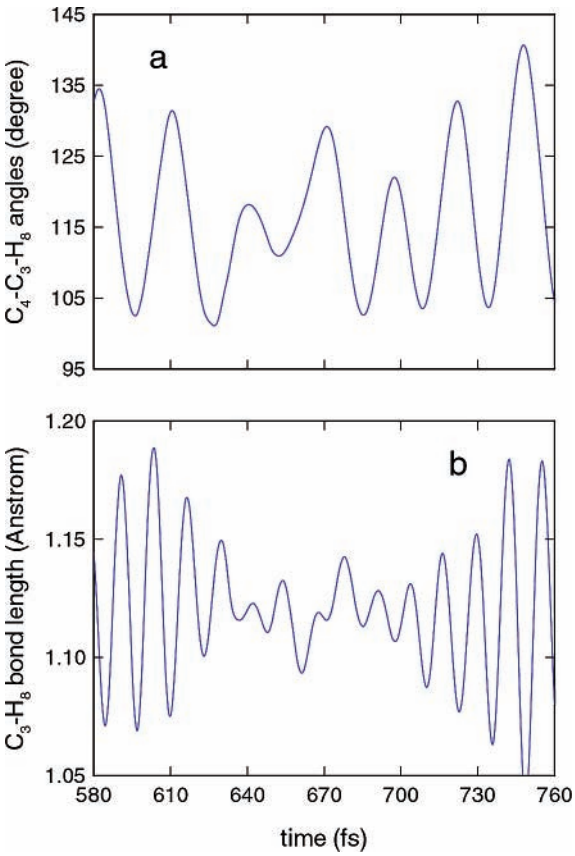

Figure 8. Expanded scale for variations in (a) $C_4-C_3-H_8$ bond-bending angle and (b) C_3-H_8 bond length.

Figure 8 shows the following for the period from 630 to 700 fs: The $C_4-C_3-H_8$ bending angle is 115°, slightly lower than

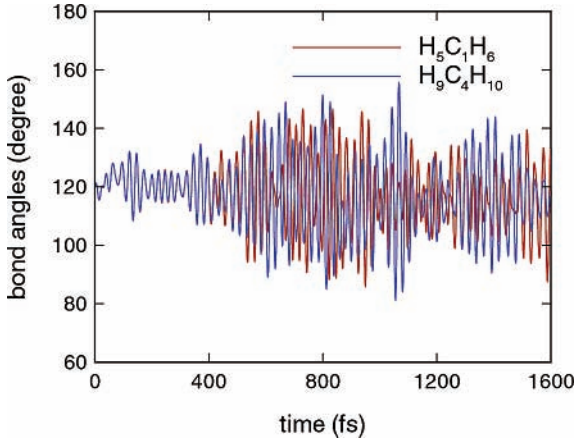

Figure 9. Variations in $H_5-C_1-H_6$ and $H_9-C_4-H_{10}$ bond-bending angles with time.

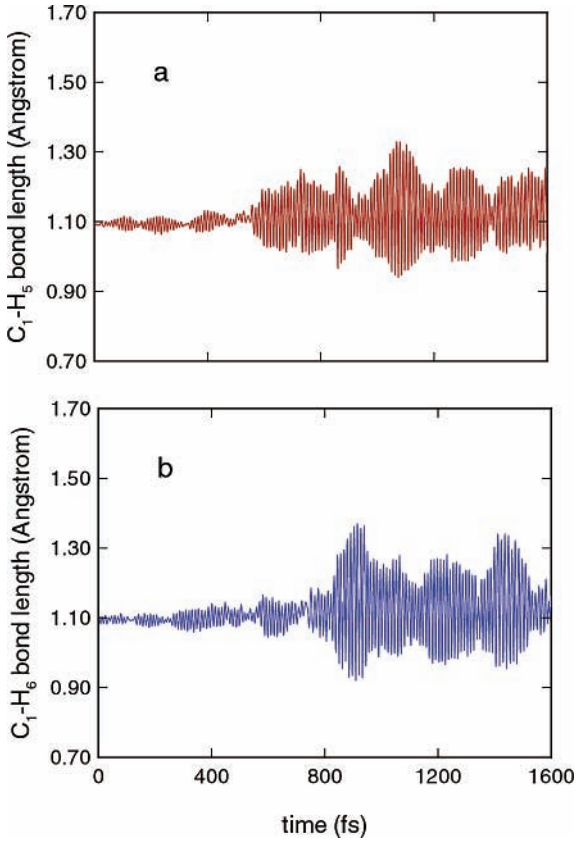

Figure 10. Variation with time of (a) C_1-H_5 bond length and (b) C_1-H_6 bond length.

its initial value of 120°; the C_3-H_8 bond length is 1.12 Å, slightly longer than its initial value of 1.10 Å; the C_3-H_8 bond stretching vibration becomes weaker. All of these results suggest moderately strong hydrogen migration couplings to the nonadiabatic transitions that occur during this period of time.

The variations of two in-plane bending angles of CH_2 groups against time are presented in Figure 9. The vibrations are initially excited by laser irradiation and further intensified after 600 fs by the electronic energy released at nonadiabatic transitions.

Variations with time of several C−H bond lengths are shown in the next two figures: C_1-H_5 and C_1-H_6 in Figure 10 and C_4-H_9 and C_4-H_{10} in Figure 11. These results suggest excitation due to vibrational energy redistribution. Correlations in the vibrational amplitudes indicate that there are processes causing energy to flow between adjacent C−H bond stretching modes.

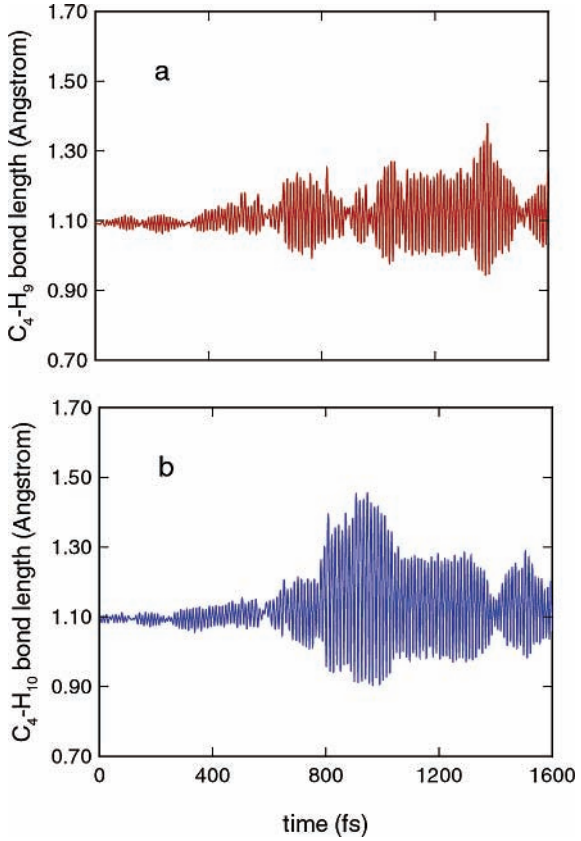

Figure 11. Variation of (a) C_4-H_9 bond length and (b) C_4-H_{10} bond length.

It is informative to monitor the electronic energy and the kinetic energy of nuclear motion, which are shown in Figure 12. The total energy of the valence electrons rises sharply in the first 150 fs, from −253.0 to −240.5 eV, as energy is absorbed from the radiation field. This quantity subsequently drops shortly after 400 fs and again after 700 fs as energy is released to atomic motion in the nonadiabatic transitions at avoided crossings that have been discussed above (two of these occur at 402 and 705 fs). The corresponding increases in nuclear kinetic energy can be observed in Figure 12b: During the first 150 fs, while the laser pulse is being applied, electrons are excited to states that provide decreased bonding, and as a result, the interatomic forces become repulsive. During this period, the nuclear kinetic energy increases from 0 to about 1 eV. There are then subsequent increases at about 400 and 700 fs as the electrons undergo downward transitions and excite atomic vibrations.

As mentioned above, numerous theoretical calculations have addressed photoisomerization of butadiene. Nonadiabatic decays induced by C−C torsions have been proposed in many studies involving both one-dimensional approximations and more accurate ab initio calculations. In particular, Robb and co-workers[24,39] studied an entire conformational space of three torsions using MC−SCF calculations. Before we compare our results with their conclusions, it is helpful to first compare the two different approaches used in these studies. The present model offers a very detailed dynamical description of the reaction process but employs an approximate Hamiltonian. On the other hand, the MC−SCF approach employed by Robb and co-workers focuses on a more accurate Hamiltonian that includes electron correlations but for which there are no dynamical calculations. Each approach is incomplete by itself, but together they provide complementary pictures for the reaction of interest here: The MC−SCF study shows that a twisting involving three

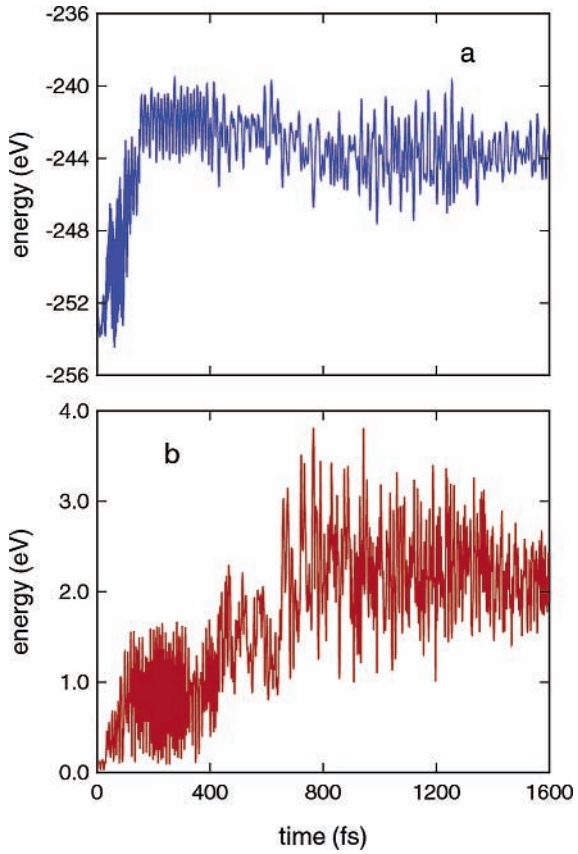

Figure 12. (a) Electronic energy and (b) kinetic energy of nuclear motion as functions of time.

C−C bonds may lead to energy degeneracy of the electronic ground state and the covalent excited state. This result forms the basis of the conical intersection mechanism proposed for nonadiabatic transitions leading to photoisomerization reaction products. The fact that no energy degeneracy of molecular orbitals is observed in the present study might be due to the use of mean field theory or may result from the strong couplings of other vibrational modes to the reaction coordinate. On the other hand, some dynamical features observed in the present study are not accessible in static MC−SCF calculations. These include the fact that nonadiabatic transitions can occur efficiently via avoided crossings with energy gaps as big as 0.6 eV and the fact that molecular twisting around two terminal C−C bonds precedes, and probably stimulates, the twisting around the central C−C bond.

IV. Summary

We have investigated trans → cis photoisomerization of butadiene, employing realistic simulations of the coupled dynamics of electrons and nuclei. The electrons are also coupled to the radiation field during the application of the laser pulse, which was taken to have a fwhm duration of 75 fs, a photon energy centered at 4.18 eV, and a fluence of 0.90 kJ/m^2.

The results of the present simulations illuminate in considerable detail the full mechanism for the trans → cis photoisomerization of butadiene following a femtosecond-scale laser pulse. After both HOMO → LUMO and LUMO → LUMO + 1 excitations, the central C−C bond and terminal C−C bonds undergo an inversion in character: The former is effectively converted from a single bond to a double bond during the first few hundred femtoseconds with a shortened length and higher-frequency vibrations, while the latter are converted from double to single bonds during this period.

The two terminal C−C bonds are thus weaker than the central C−C bond while the molecule is in the electronically excited state. The twisting of the molecule from trans to cis geometry consequently starts with rotations about these two terminal C−C bonds (through the angles ϕ_1 and ϕ_2 of Figure 1). As the molecule twists, the molecular orbital energy levels experience avoided crossings, where the electrons can undergo downward transitions by creating vibrational excitations.

After a series of such nonadiabatic decays, the electrons are essentially back in their ground state and the C−C bonds have also regained their ground-state character. Molecular rotation around the two terminal bonds is then blocked, but the molecule continues to rotate around the central C−C bond until the cis conformation is achieved.

Acknowledgment. This work was supported by the Robert A. Welch Foundation, ONR, and DARPA. The work of B.R.T. was performed under the auspices of the U.S. Department of Energy and Lawrence Livermore National Laboratory under Contract No. W-7405-Eng-48.

References and Notes

(1) Orlandi, G.; Zerbetto, F.; Zgierski, M. Z. *Chem. Rev.* **1991**, *91*, 867.
(2) Kohler, B. E. *Chem. Rev.* **1993**, *93*, 41.
(3) Leigh, W. J. In *CRC Handbook of Organic Photochemistry and Photobiology*; Horspool, W. M., Song, P.-S., Eds.; CRC Press: Boca Raton, FL, 1995; pp 123−142 and references therein.
(4) Klessinger, M.; Michl, J. *Excited States and Photochemistry of Organic Molecules*; VCH: New York, 1995; pp 336−339.
(5) Yoshizawa, T.; Wald, G. *Nature* **1963**, *197*, 1279.
(6) Wald, G. *Science* **1968**, *162*, 230.
(7) Birge, R. R. *Annu. Rev. Phys. Chem.* **1990**, *41*, 683.
(8) Jacobs, H. J. C.; Havinga, E. *Adv. Photochem.* **1979**, *11*, 305.
(9) Mcdiarmid, R.; Sheybani, A.-H. *J. Chem. Phys.* **1988**, *89*, 1255.
(10) Saltiel, J.; Sears, D. F., Jr.; Turek, A. M. *J. Phys. Chem. A* **2001**, *105*, 7569.
(11) Petek, H.; Bell, A. J.; Christensen, R. L.; Yoshihara, K. *J. Chem. Phys.* **1992**, *96*, 2412.
(12) Petek, H.; Bell, A. J.; Choi, Y. S.; Yoshihara, K.; Tounge, B. A.; Christensen, R. L. J. *J. Chem. Phys.* **1993**, *98*, 3777.
(13) Kandori, H.; Katsuta, Y.; Ito, M.; Sasabe, H. *J. Am. Chem. Soc.* **1995**, *117*, 2669.
(14) Doering, J. P.; McDiarmid, R. *J. Chem. Phys.* **1980**, *73*, 3617.
(15) Chadwick, R. R.; Gerrity, D. P.; Hudson, B. S. *Chem. Phys. Lett.* **1985**, *115*, 24.
(16) Lin, S. W.; Groesbeek, M.; van der Hoef, I.; Verdegem, P.; Lugtenburg, J.; Mathies, R. A. *J. Phys. Chem. B* **1998**, *102*, 2787.
(17) Schoenlein, R. W.; Peteanu, L. A.; Mathies, R. A.; Shank, C. V. *Science* **1991**, *254*, 412.
(18) Dobler, J.; Zinth, W.; Kaiser, W.; Oesterhelt. D. *Chem. Phys. Lett.* **1988**, *144*, 215.
(19) Cyr, D. R.; Hayden, C. C. *J. Chem. Phys.* **1996**, *104*, 771.
(20) Fuss, W.; Schmid, W. E.; Trushin, S. A. *Chem. Phys. Lett.* **2001**, *342*, 91.
(21) Ohta, K.; Naitoh, Y.; Saitow, K.; Tominaga, K.; Hirota, N.; Yoshihara, K. *Chem. Phys. Lett.* **1996**, *256*, 629.
(22) Aoyagi, M.; Osamura, Y.; Iwata, S. *J. Chem. Phys.* **1985**, *83*, 1140.
(23) Ohmine, I. *J. Chem. Phys.* **1985**, *83*, 2348.
(24) Olivucci, M.; Ragazos, I. N.; Bernardi, F.; Robb, M. A. *J. Am. Chem. Soc.* **1993**, *115*, 3710.
(25) Brink, M.; Jonson, H.; Ottosson, C.-H. *J. Phys. Chem. A* **1998**, *102*, 6513.
(26) Serrano-Andres, L.; Merchan, M.; Nebot-Gil, I.; Lindh, R.; Roos, B. O. *J. Chem. Phys.* **1993**, *98*, 3151.
(27) Ostojic, B.; Domcke, W. *Chem. Phys.* **2001**, *269*, 1.
(28) Blomgren, F.; Larsson, S. *Int. J. Quantum Chem.* **2002**, *90*, 1536.
(29) Nakayama, K.; Nakano, H.; Hirao, K. *Int. J. Quantum Chem.* **1998**, *66*, 157.
(30) Egorova, D.; Kuhl, A.; Domcke, W. *Chem. Phys.* **2001**, *268*, 105.
(31) Dormans, G. J. M.; Groenenboom, G. C.; Buck, H. M. *J. Chem. Phys.* **1987**, *86*, 4895.
(32) Perisco, M. *J. Am. Chem. Soc.* **1980**, *102*, 7839.

(33) Warshel, A.; Chu, Z. T.; Hwang, J.-K. *Chem. Phys.* **1991**, *158*, 303.
(34) Seidner, L.; Domcke, W. *Chem. Phys.* **1994**, *186*, 27.
(35) Köppel, H.; Domcke, W.; Cederbaum, L. S. *Adv. Chem. Phys.* **1984**, *57*, 59.
(36) Schneider, R.; Domcke, W.; Köppel, H. *J. Chem. Phys.* **1990**, *92*, 1045.
(37) Krawczyk, R. P.; Malsch, K.; Hohlneicher, G.; Gillen, R. C.; Domcke, W. *Chem. Phys. Lett.* **2000**, *320*, 535.
(38) Ito, M.; Ohmine, I. *J. Chem. Phys.* **1997**, *106*, 3159.
(39) Garavelli, M.; Bernardi, F.; Olivucci, M.; Bearpark, M. J.; Klein, S.; Robb, M. A. *J. Phys. Chem. A* **2001**, *105*, 11496.
(40) Garavelli, M.; Smith, B. R.; Bearpark, M. J.; Bernardi, F.; Olivucci, M.; Robb, M. A. *J. Am. Chem. Soc.* **2000**, *122*, 5568.
(41) Ben-Nun, M.; Martinez, T. J. *Chem. Phys. Lett.* **1998**, *298*, 57.
(42) Humphrey, W.; Lu, H.; Logunov, I.; Werner, H.-J.; Schulten, K. *Biophys. J.* **1998**, *75*, 1689.
(43) Berweger, C. D.; van Gunsterer, W. F.; Muller-Plathe, F. *Angew. Chem., Int. Ed.* **1999**, *38*, 2609.
(44) Zewail, A. H. *Femtochemistry: Ultrafast Dynamics of the Chemical Bond*; World Scientific: Singapore, 1998.
(45) Allen, R. E.; Dumitrica, T.; Torralva, B. R. In *Ultrafast Physical Processes in Semiconductors*; Tsen, K. T., Eds.; Academic Press: New York, 2001; Chapter 7.
(46) Torralva, B. R.; Allen, R. E. *J. Mod. Opt.* **2002**, *49*, 593.
(47) Torralva, B.; Niehaus, T. A.; Elstner, M.; Suhai, S.; Frauenheim, Th.; Allen, R. E. *Phys. Rev. B* **2001**, *64*, 153105.
(48) Dou, Y.; Torralva, B. R.; Allen, R. E. *J. Mod. Opt.*, in press.
(49) Porezag, D.; Frauenheim, Th.; Köhler, Th.; Seifert, G.; Kaschner, R. *Phys. Rev. B* **1994**, *51*, 12947.
(50) Peierls, R. *Z. Phys* **1933**, *80*, 763.
(51) Graf, M.; Vogl, P. *Phys. Rev. B* **1994**, *51*, 4940.
(52) Boykin, T. B.; Bowen, R. C.; Klimeck, G. *Phys. Rev. B* **2001**, *63*, 245314.
(53) Baughman, R. H.; Kohler, B. E.; Levy, I. J.; Spangler, C. *Synth. Met.* **1985**, *11*, 37.